Photolytic and photocatalytic removal of a mixture of four veterinary antibiotics

Johanna Zambrano [a,b], Pedro Antonio García-Encina [a,b], Juan José Jiménez [a,c], Rebeca López-Serna [a,c], Rubén Irusta-Mata [a,b,*]

[a] Institute of Sustainable Processes, University of Valladolid, Dr. Mergelina s/n, 47011 Valladolid, Spain
[b] Department of Chemical Engineering and Environmental Technology, School of Industrial Engineering, University of Valladolid, Dr Mergelina s/n, 47011 Valladolid, Spain
[c] Department of Analytical Chemistry, University of Valladolid, Campus Miguel Delibes, Paseo Belen 7, 47011 Valladolid, Spain

A B S T R A C T

The removal of a mixture of four veterinary antibiotics (VA) – tetracycline (TET), ciprofloxacin (CIP), sulfadiazine (SDZ) and sulfamethoxazole (SMX) – via photo-degradation (UVC) and photocatalysis with TiO_2 (UVC/ TiO_2) was investigated in a batch reactor under different initial concentrations (20, 100, 500 and 1000 µg/L per antibiotic). Ultra-high performance liquid chromatography coupled to a mass spectrometry (UHPLC-MS/MS) was used to determine the removal of these veterinary antibiotics. The removal of all antibiotics via photolysis was around 98–99% after 100 h for TET, 122 h for CIP, 212 h for SDZ and 240 h for SMX. Nevertheless, the removal of all antibiotics via photocatalysis was around 99–100% after 4.2 h for TET, 3.5 h for CIP, 7.1 h for SDZ and 16.5 h for SMX. The photolysis for the four veterinary antibiotics followed a first-order irreversible kinetic model. The photocatalysis of TET, CIP and SDZ followed a Langmuir-Hinshelwood kinetic model, and adsorption was considered the limiting step. SMX followed a first-order irreversible kinetic model. The photolytic degradation rate constant (k_1) was 0.00073 min^{-1} for TET, 0.00055 min^{-1} for CIP, 0.00031 min^{-1} for SDZ and 0.00027 min^{-1} for SMX. While for photocatalysis k_1 was 0.0044 min^{-1} for SMX; k_{L-H} was 0.0284 min^{-1} for TET, 0.0379 min^{-1} for CIP and 0.0141 min^{-1} for SDZ. The VA degradation was enhanced by the use of a catalyst. Additionally, electrical energy per order (E_{EO}) was assessed to estimate the electrical energy efficiency of each process. E_{EO} values for photolysis were 339.06 kWh/m^3/order for TET, 449.84 kWh/m^3/order for CIP, 795.31 kWh/ m^3/order for SDZ and 897.71 kWh/m^3/order for SMX. On the other hand, E_{EO} values for photocatalysis were 14.96 kWh/m^3/order for TET, 12.07 kWh/m^3/order for CIP, 20.39 kWh/m^3/order for SDZ and 62.10 kWh/m^3/ order for SMX. The energy consumption for photocatalysis was considerably lower than for photolysis. This study determined an overall degradation rate constant for a wide range of TET, CIP, SDZ and SMX concentrations. Furthermore, when working with a pH of 8 (a typical pH from wastewater from livestock farms) and a VA mixture whose concentrations resemble the characteristics of real water samples, that photolysis and photocatalysis are potential processes for wastewater treatment with low energy consumption.

1. Introduction

Antibiotics are one of the most important pharmaceutical groups used by humans and are also used in veterinary medicine and aquaculture. Veterinary antibiotics (VA) are widely used to increase animal production and prevent, control or treat diseases [1,2]. The widespread use of antibiotics means that they are commonly found in wastewater, surface water, ground water, and drinking water at trace concentration levels, ranging from ng/L to mg/L. The presence of VA in aquatic environments has become an increasing global concern due to their potential adverse effects to the environment and significant public health implications [3].

Treatment technologies available for VA include biological processes and/or physical or chemical treatments. Biological processes which use aerobic or anaerobic sludge [4], microalgae [5], algal-bacterial consortium [6], among others, are cost-efficient; however, some VA can

inhibit the regular function of microbial populations due to their toxicity and microbial growth resistance. On the other hand, chemical process such as coagulation [7] or ion exchange [8] present low efficiency, high cost, and secondary pollution issues. Similarly, physical processes such as activated carbon [9] and other adsorption techniques with carbon-based material or metal oxides [10], despite their corrosion resistance, high reactivity and low price; they cannot eliminate VA since they only transfer the pollutants from one phase to another [11].

The growing interest in VA has led to extensive studies on environmentally friendly processes which can be cost effective. Over the last few years, advanced oxidation processes (AOPs) such as ozonation [12,13], Fenton oxidation [14–16], electrochemical degradation [17–20], photolysis and photocatalysis [21–23] had been widely studied for wastewater treatment. Specially, ultraviolet (UV) irradiation has demonstrated its effectiveness for chemical oxidation and water and wastewater disinfection. Direct and natural photolytic decomposition and transformation of many organic pollutants has been proved [24]. Moreover, photocatalysis has emerged as a promising technique for VA removal as it can mineralize a variety of recalcitrant organics through the generation of hydroxyl radical (OH$^\bullet$) which is highly reactive and non-selective [25]. Titanium dioxide (TiO_2) is the most widely used catalyst due to its abundance, photo stability, good performance and non-toxic characteristics [26]. In addition, several authors [27–29] have shown that TiO_2 can be reused because photocatalytic activity and catalysts remain almost unchanged after several cycles. The reuse of TiO_2 can reduce operating costs and promote the competitiveness of photocatalysis among other wastewater treatment processes [22,30].

Photocatalytic processes have shown to be a suitable choice because they can obtain high mineralization percentages. However, most of the previous studies found in the literature have focused on a single contaminant which may not be representative of real water treatment conditions [31]. From this perspective, the aim of this study is to determine the photolytic and photocatalytic degradation of a mixture of TET, CIP, SDZ and SMX, as representative compounds of fluoroquinolones, sulfonamides and tetracyclines, the three antibiotic families most frequently found in piggery water samples, at small concentrations similar to those found in real samples.

To determine the influence of the initial concentration on the photolytic (UVC) and photocatalytic (UVC/TiO_2) degradation of TET, CIP, SDZ and SMX, four different initial concentrations (20, 100, 500 and 1000 µg/L) of each compound were used. These concentrations were selected to resemble a range of VA concentrations in manure which can be found in the literature (sulfonamides 6.99–5650 µg/kg, fluoroquinolones 63.63–5567 µg/kg, and tetracyclines 6.20–290.5 µg/kg [32]). To our knowledge, no other authors have published rate constants for TET, CIP, SDZ and SMX by fitting experimental data over a wide range of concentrations to a single general equation. In the literature is common to find studies with different initial VA concentration and a rate constant for each concentration, which is not correct, because when the other operating parameters do not change, the rate constant does not change with concentration. Removals, kinetics and energy consumption were studied and compared with the literature. Other important parameters which can influence the efficiency of the process – such us pH, light intensity, type of radiation, use of O_2, and irradiation time – remained unchanged during the operation time. However, they were considered in the comparison with the literature.

2. Materials and methods

2.1. Chemicals and reagents

Individual stock solutions of 1 g/L for TET, SDZ and SMX were prepared on a weight basis in methanol (MeOH). CIP was dissolved in H_2O/MeOH (1:1) containing 0.2% *v/v* hydrochloric acid (HCl). MeOH of high analytical grade was acquired from Sigma-Aldrich (Stockholm, Sweden), VA of high purity grade (N95%) and HCl (37%) were obtained

from Sigma-Aldrich (Tres Cantos, Madrid, Spain). CIP, SDZ and SMX were acquired as neutral non-solvated molecules and TET was purchased as a hydrochloride. P-25 titanium dioxide (Degussa AG, Germany) was supplied by Quimidroga S.A. TiO_2 specific surface was 50 ± 15 m^2, the particle size was 21 nm and the bandwidth energy was 3.2 eV. Ultrapure water was generated by a Milli-Q (MQ) Advantage Ultrapure Water purification system and filtered through a 0.22 µm Millipak Express membrane and an LC-Pak polishing unit by Merk Millipore (Billercia, MA, USA).

2.2. Experimental set-up

The photoreactor system (Fig. 1) consists of a methacrylate reactor formed by two concentric tubes. The outer tube has an inner diameter of 14 cm and the inner tube has an outer diameter of 6 cm. These measurements have been designed so that the wall of the inner tube to the outside does not exceed 4 cm in order to avoid loss of radiant energy. The active zone in the reactor is delimited by the two tubes and the liquid level, which has a useful volume of 5.6 L. Philips UVC lamp (TUV PL-L 36W/4P 1CT/25) with a peak emission at 257.7 nm and TiO_2 in suspension were used. A homogeneous incident flux of 13.33 mW/cm^2 was used. A cylindrical shape diffuser placed at the bottom of the reactor, which injected air from a diaphragm pump, was used for a continuous mixing.

2.3. Degradation analysis

Photolytic and photocatalytic degradation experiments were performed under UVC irradiation at 25 °C and a pH of 8.0. Tests were performed with a mixture of four antibiotics to a final concentration of 1000, 500, 100 and 20 µg/L per antibiotic. After filling the reactor, for the photolytic analysis, an initial sample was taken to determine the initial antibiotic concentration and the UVC lamp was immediately turned on. For the photocatalytic analysis, an initial sample was taken to determine the initial antibiotic concentration. After that, TiO_2 was added to the reactor under continuous mixing to obtain a concentration of 1 g/L. The solution was stirred under dark conditions for 30 min and two samples were taken every 15 min. The available literature was revised and determined 30 min as an optimal time to reach a point in which adsorption is not the dominant process in the removal of VA [1,26,33]. Moreover, from an applied engineering point of view, it
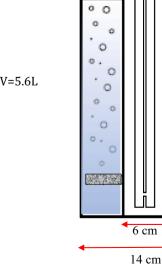

Fig. 1. Photoreactor system scheme.

would not make sense to keep the solution stirring under dark conditions for a longer time to reach equilibrium, as photocatalysis is a process that occurs in hours or less. After 30 min the UVC lamp was switched on and samples were taken at prefixed intervals, filtered through 0.22 mm pore-size nylon syringe filters (Fisherbrand) and stored at 4 °C before analysis. Experiments were conducted in triplicate.

2.4. Analytical method

The quantitative determination of selected antibiotics was carried out by ultra-high performance liquid chromatography (UHPLC) coupled to a MS/MS spectrometry. The chromatographic separation was carried out using an Exion LC AD instrument from AB Sciex (Framingham, MA, USA) and a reversed-phase column EVO C18 (50 × 2.1 i.d. mm, 1.7 μm particle size) from Phenomenex (Torrance, CA, USA). MS/MS analysis was performed by a triple quadrupole 6500+ from AB Sciex in selected reaction monitoring (SRM) mode. The procedure was based on the one previously developed by López-Serna et al. [34], employing direct injection of the (diluted) samples, without any pre-concentration step.

2.5. Zero-point charge (ZPC)

pH plays a significant role in VA photocatalytic degradation in regards to the surface charge properties of the catalyst, the size of the catalyst aggregates, the adsorption of VA on the catalyst surface, the ionic forms of the VA, and hydrophobicity [11,25,30]. Regarding to the surface charge properties and the particle size of the catalyst, the pH_{ZPC} is the pH at which the catalyst surface is globally neutral; consequently, the electrostatic attraction between the photocatalyst particles and the VA is minimal. Above the zero-point charge (ZPC) value, the catalyst surface will be negatively charged and will repel the negatively charged VA. Below the ZPC value, the catalyst surface will be positively charged and will exert an electrostatic force towards the anionic compounds.

To calculate pH_{ZPC}, 50 mL of Milli-Q water were taken in 100 mL glass beakers, adjusting the pH between 3 and 11 by adding the appropriate amount of 0.1 M HCl or 0.1 M NaOH. After that, 0.5 g of TiO_2 were added to each glass beaker, and the final pH values were measured after 48 h under stirring at room temperature. The values of the final pH were plotted versus the initial pH. The pH_{ZPC} corresponds to the point where the curve of the final pH versus the initial pH cuts the graph diagonally [35].

2.6. Kinetic analysis

Four kinetic models – zero-order (Eq. (1)), pseudo-first order irreversible (Eq. (2)), pseudo-first order reversible (Eq. (3)) and Langmuir-Hinshelwood (Eq. (4)) – were used to fit the experimental data.

$$r = -\frac{dC}{dt} = k_0 \tag{1}$$

$$r = -\frac{dC}{dt} = k_1 \cdot C \tag{2}$$

$$r = -\frac{dC}{dt} = k_2 \cdot (C - C_e) \tag{3}$$

$$r = -\frac{dC}{dt} = \frac{k_r \cdot K \cdot C}{1 + K \cdot C} \tag{4}$$

where, r is the rate of antibiotics degradation ($\mu g \cdot L^{-1} \cdot min^{-1}$), C is the concentration at any time ($\mu g \cdot L^{-1}$), C_e is the concentration at equilibrium ($\mu g \cdot L^{-1}$), k_0 is the zero-order rate constant ($\mu g \cdot L^{-1} \cdot min^{-1}$), k_1 is the pseudo-first order irreversible rate constant (min^{-1}), k_2 is the pseudo-first order reversible rate constant (min^{-1}), and k_r ($\mu g \cdot L^{-1} \cdot min^{-1}$) and K ($L \cdot \mu g^{-1}$) are the rate constant and the adsorption constant, respectively.

Integrating Eqs. (1), (2), (3) and (4) with respect to the limits $C = C_0$ (C_0 is the initial antibiotic concentration before irradiation and after 30 min to reach the adsorption equilibrium when TiO_2 is used) and $C = C_t$ (C_t is the antibiotic concentration at time t (min) under light irradiation), Eqs. (5), (6), (7) and (8) can be obtained:

$$C_t = C_0 - k_0 \cdot t \tag{5}$$

$$C_t = C_0 \cdot e^{-k_1 \cdot t} \tag{6}$$

$$C_t = C_e + (C_0 - C_e) \cdot e^{-k_2 \cdot t} \tag{7}$$

$$-ln\left(\frac{C_t}{C_0}\right) - K \cdot (C_t - C_0) = k_r \cdot K \cdot t \tag{8}$$

Eq. (6) is a particular solution of Eq. (7) when $C_e = 0$; thus, the pseudo-first order kinetics is not reversible.

2.7. Electrical energy determination

In order to compare photocatalysis by means of energy consumption with other advanced oxidation processes (AOP), the electrical energy per order (E_{EO}) was calculated. E_{EO} is defined as the electrical energy required to reduce the concentration of a pollutant by one order of magnitude (90%) in a fixed volume of polluted water. E_{EO} is calculated as follows:

$$E_{EO} = \frac{P \cdot t}{V \cdot log\left(\frac{C_0}{C_f}\right)} \tag{9}$$

where, P is the rated power (kW) of the AOP system, V is the volume (m^3) of water treated in the time t (h), C_0 ($\mu g/L$) is the initial antibiotic concentration before irradiation (and after 30 min to reach the adsorption equilibrium when TiO_2 is used), and C_f ($\mu g \cdot L^{-1}$) is the final antibiotic concentration.

3. Results and discussions

3.1. Zero-point charge (ZPC)

Several authors have reported the ZPC of TiO_2 in the pH range of 4.5 to 7.0 [30]. In the preset study, pH_{ZPC} for TiO_2 was found at pH 6.4 (Fig. 2). Therefore, since the present study was performed at pH 8 to resemble pH of real water samples, the photocatalyst was negatively charged.

Considering the pH of the solution, the VA pK_a, and the pH_{ZPC} of TiO_2, the following predictions of the different interaction mechanisms can be made. The four antibiotics used in the present study can exist as three different species (ionic, cationic and zwitterionic) over a broader pH range. TET with $pK_{a1} = 3.32$ and $pK_{a2} = 9.58$ will be in its zwitterionic form and present hydrophobic interactions with the photocatalyst that will be negatively charged [36]. CIP pK_a is 6.09 for the carboxylic acid group and 8.74 for the nitrogen on the piperazinyl ring. The acid will be dissociated at pH values higher than 6.3, and the nitrogen will be protonated at pH values lower than 8.7. At pH 8.0, CIP will be dissociated in anions and cations. Through electrostatic attraction, cations will be adsorbed on the negatively charged TiO_2 [37]. SDZ pK_a is 6.36 and SMX pK_a values are $pK_{a1} = 1.6$ and $pK_{a2} = 5.7$. At pH 8.0, SDZ and SMX (pH > pK_a; pH_{PZC} < pH) will be negatively charged which will cause an electrostatic repulsion with negatively charged TiO_2 [36].

3.2. Degradation of veterinary antibiotics

To the best of our knowledge, for the first time, a mixture of four antibiotics with an initial concentration range adjusted to those that can be found in real water samples was used to analyze the degradation of VA via photolysis and photocatalysis. VA photolysis was studied in batch
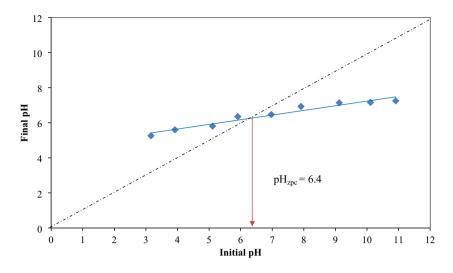
Fig. 2. Evaluation of zero-point charge (pH_{zpc}) for TiO_2.

experiments for 180 min (Fig. 3A–D). For the four antibiotics, a decrease in the initial concentration over time was observed. In all the studied conditions, TET showed a higher decrease in its initial concentration because it is a very light sensitive antibiotic. In a literature review, Prakash et al., [38] compared the photolysis of tetracyclines, quinolones and sulfonamides, and showed that tetracyclines can obtain high removals, around 80%, while quinolones and sulfonamides achieve very low removals.

Moreover, photocatalysis was evaluated for 180 min (Fig. 4A–D). Starting with an initial VA concentration of 100 μg/L before adsorption, complete removal of TET was obtained at 180 min and at 90 min CIP was totally removed (Fig. 4C). At 20 μg/L before adsorption, complete removal of TET and CIP was obtained at 75 and 60 min, respectively (Fig. 4D). In all the studied conditions, CIP showed the highest decrease in its initial concentration. Considering the pH_{ZPC} and pH solution, CIP was dissociated – hence its cations enhanced its adsorption capacity on the negatively charged TiO_2 through electrostatic attraction [39]. Adsorption into the catalyst is crucial to obtain high removal percentages. In the following sections, we will determine the kinetics of the photolytic and photocatalytic processes as well as the removal percentages than can be obtained by these processes.

3.3. Kinetics of degradation of veterinary antibiotics

The photolysis and photocatalysis of the four veterinary antibiotics were investigated with zero-order and pseudo-first order kinetic models. A pseudo-first order kinetic model was evaluated and considered both an irreversible and a reversible reaction. It was considered that the photolytic and the photocatalytic reaction could reach an equilibrium where parental compounds and byproducts generated during the process would compete for the photons, electron holes produced on the catalyst and/or the generated oxidation species. Additionally, the Langmuir-Hinshelwood kinetic model, which considered adsorption as the limiting step, was used to study the kinetics of photocatalysis. To calculate the kinetic parameters of photocatalysis, the experimental data was considered after adsorption when the UVC light was turned on.

The kinetic parameters were obtained as follows (Table 1):

1. An adjustment of the experimental data to a zero-order kinetic was done as shown in Eq. (5) by drawing the concentration data versus time. If the kinetics is a zero-order, then the experimental data will fit to a straight line with the ordinate at the origin C_0 and slope -k_0.
2. Analogously transforming Eq. (6), Eq. (9) is obtained:

$$-ln\left(\frac{C_t}{C_0}\right) = k_1 \cdot t \tag{9}$$

By drawing $-ln(C_t/C_0)$ versus t, if the kinetics is a pseudo-first order irreversible, then the experimental data will fit to a straight line with the ordinate at the origin C_0 and slope k_1.

3. The experimental data was also fitted to a pseudo-first order reversible kinetics by transforming Eq. (7) into

$$-ln\left[\frac{C_t - C_e}{C_0 - C_e}\right] = k_2 \cdot t \tag{10}$$

By drawing $-ln[(C_t - C_e)/(C_0 - C_e)]$ versus t, if the kinetics is a pseudo-first order reversible, then the experimental data will fit to a straight line with the ordinate at the origin and slope k_2. For this, we must find the values of parameters k_2 and C_e which would make the experimental data fit best to that straight line. Those parameters were obtained by the GRG Nonlinear Solving method.

4. Fitting experimental data of photolysis and photocatalysis as in step 3, the C_e obtained was 0, it means that the kinetic model that best fit was the pseudo-first order irreversible model.

5. Additionally, for photocatalysis, when the experimental data was fitted to a pseudo-first order irreversible kinetic model at small antibiotic concentrations, the experimental data started to disperse from the line. Therefore, we inferred that the photocatalysis of the antibiotic might be limited by the adsorption of the antibiotics into the catalyst and that the photocatalytic process might follow a Langmuir-Hinshelwood kinetics [20,35].

Once again, the best values of the constants k_r and K in Eq. (8) were obtained using the GRG Nonlinear Solving method.

6. The coefficient of determination R^2 was used to decide whether the experimental data better fit a zero-order, pseudo-first order irreversible/reversible, or Langmuir-Hinshelwood kinetics model.

3.3.1. Photolysis

Pseudo-first order irreversible kinetics presented R^2 values closer to unity and fit best to the experimental data for the photolysis of TET, CIP, SDZ and SMX (Fig. 5). TET and CIP were degraded faster than SDZ and SMX. TET presented the higher rate constant in the photolytic process. The pseudo-first order irreversible rate constant for the removal of antibiotics by photolysis were 0.00073 min^{-1} for TET, 0.00055 min^{-1} for CIP, 0.00031 min^{-1} for SDZ and 0.00027 min^{-1} for SMX.
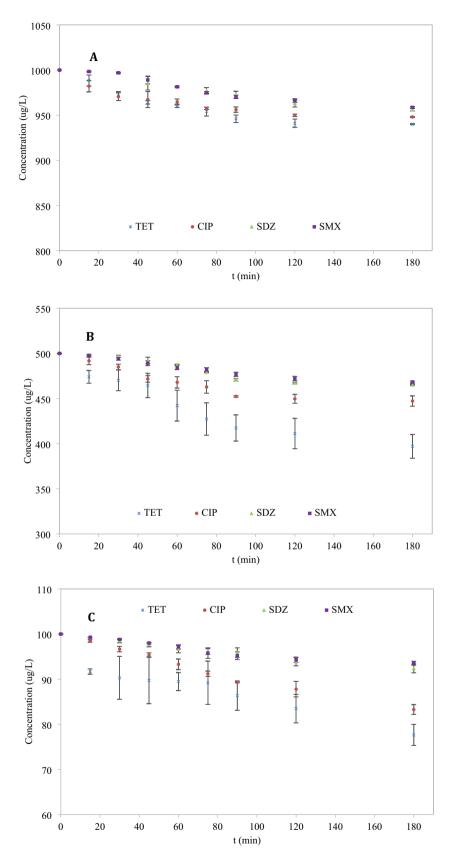
Fig. 3. Antibiotic removal by photolysis (A) 1000, (B) 500, (C) 100, and (D) 20 μgL^{-1} initial concentration. Error bars represent $\pm$ standard error of the mean.
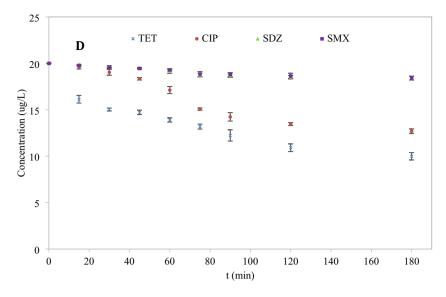
Fig. 3. (*continued*).

A comparative analysis of the rate constants previously reported in the literature for TET, CIP, SDZ and SMX degradation by photolysis showed that the results obtained in the present study are comparable to those reported by other authors (Table 2). Wu et al. [33] reported negligible photolysis of TET using UV irradiation. Yun et al. [42] found higher photolytic rate constants (0.0045–0.0014 min^{-1}) than the ones obtained in the present study, despite its higher initial TET concentration and its lower UV light intensity. The light source was not specified so no further comparison can be made. Li and Hu, [43] obtained a k_1 value of 0.01 min^{-1} for photolytic degradation which was higher than the k_1 value obtained in the present study (0.00073 min^{-1}). The reactor used by Li and Hu, [43] was a 100 mm × 50 mm dish which allows for easier light irradiation into the solution.

In another study, Li and Hu, [44] obtained higher rate constants for CIP removal than the ones obtained in the present study (0.0005 min^{-1}), due to the reactor design used by Li and Hu, [44] which was shorter and the separation of the reactor surface with the lights was 2 cm. Salma et al. [1] reported a higher rate constant of 0.002 min^{-1} for photolysis by using UVC light, as we did in the present study, but the irradiance was not specified. Triquet et al. [45] achieved a higher rate constant of 0.003 min^{-1} for photolysis, but the UV type was not specified so no further comparison can be made. Nevertheless, the present results corroborate what Triquet et al. [45] stated which was that CIP could be degraded by both techniques, photolysis and photocatalysis, with faster kinetics while using a photocatalyst.

Loureiro dos Louros et al. [46] studied the photodegradation of SDZ by UVC light, obtaining a rate constant of 0.002 min^{-1} which was higher than that obtained in the present study k_1 (0.00031 min^{-1}). This is because Loureiro dos Louros et al. [46] used tubes with small internal diameters as reactors which facilitates the light irradiation into the solution. Li et al. [21] obtaining a higher rate constant (0.02 min^{-1}) than the one obtained in the present study for photolysis degradation of SDZ due to the use of a lower pH; they determined that the higher the acidity, the greater the rate constant. Yadav et al. [47] analyzed the degradation of SDZ, achieving a photolysis rate constant of 0.001 min^{-1} which was higher than the one obtained in the present study; UVC light was used too, but the light irradiation and pH conditions were not specified.

Wang et al. [48] studied the photolytic degradation of SMX and obtained a k_1 value of 0.002 min^{-1} which was higher than the one obtained in the present study (0.00027 min^{-1}) due to the use of a high sunlight irradiance. Additionally, Yuan et al. [26] studied the degradation of SMX under UVC irradiation and achieved a higher k_1 value of 0.03 min^{-1} due to the photocatalytic system used, which were small

dishes with a high surface area and a small depth, allowing for better light irradiation into the solution.

3.3.2. Photocatalysis

The Langmuir-Hinshelwood kinetics model best fit to the experimental data for the photocatalysis of TET, CIP and SDZ (Fig. 6). CIP had the highest rate constants of the four antibiotics. CIP removal was faster than the other three antibiotics in photocatalysis due to its better absorption into the catalyst; the log K_{ow} of CIP (1.32) was higher than that of TET (−1.37), SDZ (−0.09) and SMX (0.89), indicating that CIP has a better affinity to TiO$_2$. When applying the Langmuir-Hinshelwood kinetics model to SMX, the K (constant for adsorption) obtained was 0, which means that SMX photocatalysis was not limited by adsorption. SMX followed a first-order irreversible kinetic model with a k_1 of 0.0044 min^{-1}.

Several researchers have simplified the Langmuir-Hinshelwood model by considering the term K·C << 1. Thus, the model can be simplified and takes the form of a pseudo-first order kinetics. From Table 1, k_r from the Langmuir-Hinshelwood kinetics has different units than k_1 from a pseudo-first order kinetics. Thus, it is not appropriate to approximate Langmuir-Hinshelwood kinetics to a pseudo-first order model as reported in the literature [41,45]. However, the product of $k_r·K$ gives a constant k_{L-H} with the same units (min^{-1}) of a pseudo-first order kinetic, which we will use for comparison purposes. In this respect, k_{L-H} for the removal of antibiotics by photocatalysis was 0.0284 min^{-1} for TET, 0.0379 min^{-1} for CIP and 0.0141 min^{-1} for SDZ.

Wu et al. [33] reported photocatalytic rate constants of 0.02–0.04 min^{-1} for TET degradation, similar to the one obtained in this study (0.0284 min^{-1}). Li and Hu, [43] obtained a higher k_1 value of 0.1 min^{-1} due to the pH of the solution. According to the pH$_{ZPC}$ of TiO$_2$, the catalyst is positively charged under pH 6.4 and negatively charged above pH 6.4 [49]. Since in the present study the pH was 8, TET will be negatively charged and thus there will be electron repulsion with the catalyst. Furthermore, Li and Hu, [43] showed that by using a pH of 6 that TET will be in its zwitterion form and therefore a better adsorption between the antibiotic and the catalyst will improve photocatalytic degradation [50].

Li and Hu, [44] obtained higher rate constants for CIP removal of 0.22 min^{-1} than the one obtained in the present study (0.0379 min^{-1}) by using UVA light. Salma et al. [1] reported a smaller rate constant of 0.006 min^{-1} using UVC because they used a pH of 3. At pH 3, according to the pH$_{ZPC}$ of TiO$_2$ and pKa of CIP, CIP and TiO$_2$ will be positively charged and there will be electrostatic repulsion between them. Triquet
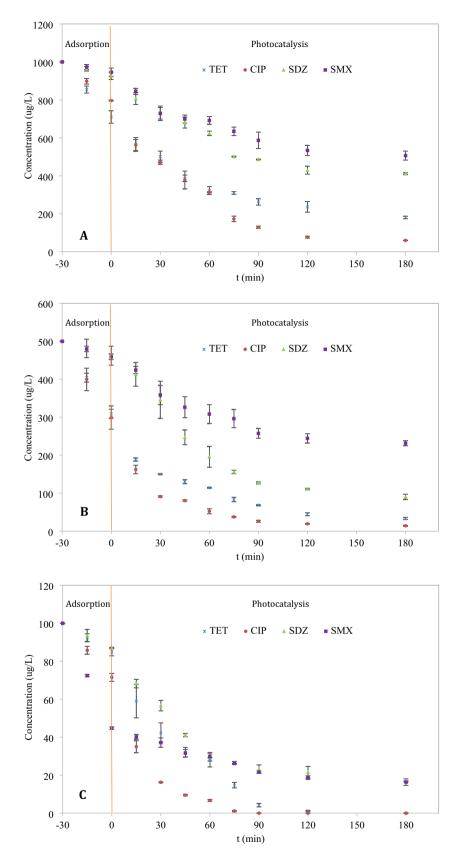
Fig. 4. Antibiotic removal by photocatalysis (A) 1000, (B) 500, (C) 100, and (D) 20 μgL^{-1} initial concentration. Error bars represent ± standard error of the mean.
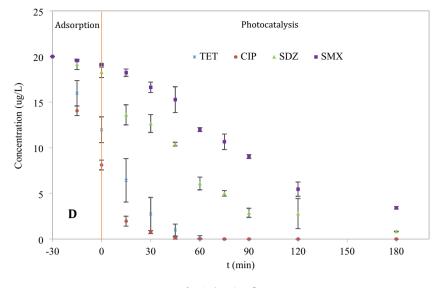
Fig. 4. (*continued*).

et al. [45] achieved a higher rate constant of 0.06 min^{-1} for CIP photocatalysis because a small narrow reactor was used which facilitates the light irradiation into the solution.

For SDZ removal, Yadav et al. [47] achieved a photocatalysis rate constant of 0.01 min^{-1} like the one obtained in the present study (0.0141 min^{-1}). It is important to mention that the rate constants of the antibiotics in the current study might be enhanced by the use of air for mixing the solution; dissolved oxygen (DO) trap photogenerated electrons, prevent charge carrier recombination, act as an electron scavenger and enable the formation of superoxide and reactive oxygen species (ROS) [30,51].

Yuan et al. [26] achieved k_1 values of 0.1 to 0.5 min^{-1} for photocatalysis degradation of SMX while using 0.4 to 1.6 g/L TiO$_2$ photocatalysis. The higher rate constants obtained by Yuan et al. [26] than the one obtained in the present study (0.0044 min^{-1}) can be explained by the pH difference. According to SMX pKa values, when the solution pH is higher than 5.6, SMX will be in its anionic form, while when the pH is between 1.85 and 5.6, SMX will be in its neutral form. Boreen et al. [52] stated that the neutral, rather than the anionic form, is the most photodegradable state. At the neutral state, SMX could obtain stronger light adsorption, corresponding to higher photochemical reactivity. Thus, the decomposition rate will decrease as the pH increases [13,40,44].

3.4. Removal of veterinary antibiotics

The removal of the four veterinary antibiotics by photolysis is shown in Fig. 5B, while their removal by photocatalysis can be seen in Fig. 6B. TET removal by photolysis was 99% after 100 h and TET removal by photocatalysis was 99.75% after 4.2 h. Wu et al. [33] studied the degradation of 10 mg/L of TET with a 20 mW/cm^2 visible light irradiation. After 150 min, no photolysis was observed. However, while using 0.2 g/L TiO$_2$, 76.6% removal was obtained. Moreover, when UV instead of visible light was used for the photocatalysis process, 94.8% of TET was removed. Safari et al. [53], using an initial concentration of 1 g/L TiO$_2$, 55 mg/L TET and 2.5 mW/cm^2 UV irradiation, achieved 23.8% and 83.2% for photolysis and photocatalysis degradation, respectively. Oseghe and Ofomaja, [54] investigated the degradation of 5 mg/L TET under 4.6 mW/cm^2 visible white LED light irradiation, attaining 26% photolysis and 40% photocatalysis removal. Comparing these reviewed studies with the results obtained in the present study, the findings agree on the capacity of photolysis and photocatalysis to degrade TET, with enhanced degradation when using a catalyst and UV irradiation.

CIP removal by photolysis was 98.7% after 122 h and CIP removal by photocatalysis was 99.90% after 3.5 h. Other studies have reported the same trend for CIP as the ones observed in the present study; photo degradation by UV irradiation and complete removal of CIP by the use of TiO$_2$ powder. Mondal et al., [55] achieved 60% removal of 10 mg/L CIP by UVC irradiation after 120 min. Salma et al., [1] found a photolytic and photocatalytic removal of 33% and 58%, respectively, for 0.02 μg/L CIP under UVC irradiation. Triquet et al., [45] by using 10 mW/cm^2 UV irradiation for the degradation of 20 mg/L CIP, obtained a complete removal of CIP after 8 h by photolysis and 1 h by photocatalysis.

SDZ removal by photolysis was 98.1% after 212 h and SDZ removal by photocatalysis was 99.61% after 7.1 h. SDZ is very stable and little degradation was observed in the absence of TiO$_2$. However, SDZ proved to be photosensitive and further degradation can be obtained by photocatalysis [56]. The results for SDZ are consistent with previous findings in the literature. Loureiro dos Louros et al. [46] reached 100% removal of 500 μg/L SDZ after 36 h of UV photolysis, and after 5 h of operation, the removal was around 25%. Yadav et al. [47] used UVC irradiation for the removal of 1 mg/L SDZ, obtaining 20% removal by photolysis after 180 min, and 55% removal by photocatalysis after 120 min. Li et al. [21] used UV irradiation for the removal of 1.5 mg/L SDZ, obtaining 95% removal after 150 min.

SMX removal by photolysis was 98.2% after 240 h and SMX removal by photocatalysis was 98.84% after 16.5 h. The SMX results are comparable with those from the literature; photolysis and photocatalysis demonstrated their ability to degrade SMX, with a higher removal when using TiO$_2$. Alharbi et al. [57] studied the degradation of 5 mg/L SMX, obtaining a complete removal after 8 min under 1.04 W/cm^2 UV irradiation. For the degradation of 200 μg/L SMX, Yuan et al. [26] achieved 53.6 to 91% removal by using 0.4 to 1.6 g/L TiO$_2$ under 0.5 mW/cm^2 UVC irradiation after 16 min. Cai and Hu, [2] analyzed the degradation of 400 μg/L SMX using 4.32·10^3 mWs/cm^2 UV energy irradiation, and reached 16% removal by photolysis and 91% removal by photocatalysis with 0.05 g/L TiO$_2$ and pH 5.6 after 20 min.

3.5. Energy consumption

The electrical energy consumption for the photolytic and photocatalytic degradation of the veterinary antibiotics was calculated. The E_{EO} values for photolysis were 339.06 kWh/m^3/order for TET, 449.84 kWh/m^3/order for CIP, 795.31 kWh/m^3/order for SDZ, and 897.71 kWh/m^3/order for SMX. SMX turned out to be the antibiotic which consumed more energy for its degradation. Likewise, for the

Table 1
Kinetic parameters for the photolysis and photocatalysis of veterinary antibiotics.

Compound	Photolysis Zero order C_o (μg/L)	k_0 (μg·L⁻¹·min⁻¹)	R^2 (-)	First Order Irreversible k_1 (min⁻¹)	R^2 (-)	Reversible[a] C_e (μg/L)	k_2 (min⁻¹)	R^2 (-)	Photocatalysis Zero order C_o (μg/L)	k_0 (μg·L⁻¹·min⁻¹)	R^2 (-)	First order Irreversible k_1 (min⁻¹)	R^2 (-)	Reversible[a] C_e (μg/L)	k_2 (min⁻¹)	R^2 (-)	Langmuir-Hinshelwood k_r (μg·L⁻¹·min⁻¹)	K (L·μg⁻¹)	R^2 (-)
TET	1000	0.199	0.79	0.00073	0.99	0	0.00073	0.99	710	3.781	0.82	0.0148	0.99	0	0.015	0.99	11.137	0.00255	0.98
CIP	1000	0.162	0.82	0.00055	0.99	0	0.00055	0.99	771	2.781	0.77	0.0194	0.98	0	0.019	0.98	15.040	0.00252	0.97
SDZ	1000	0.092	0.59	0.00031	0.99	0	0.00031	0.99	927	2.908	0.79	0.0089	0.98	0	0.009	0.98	19.776	0.000713	0.98
SMX	1000	0.082	0.83	0.00027	0.99	0	0.00027	0.99	946	1.113	0.86	0.0044	0.99	0.02	0.005	0.96	–	0	–

[a] Reversibility is not detected (C_e = 0).

photocatalytic process, SMX presented the highest E_{EO} value. The E_{EO} values for photocatalysis were 14.96 kWh/m³/order for TET, 12.07 kWh/m³/order for CIP, 20.39 kWh/m³/order for SDZ, and 62.10 kWh/m³/order for SMX. The faster photolysis rate of TET and the higher photocatalytic rate of CIP means that they are the antibiotics with the lowest electrical energy consumption in each process. E_{EO} values for photolysis were around 15 to 37 times higher than the E_{EO} values for photocatalysis.

A literature review of E_{EO} for the degradation of TET, CIP, SDZ and SMX displayed a diverse range of values (Table 3). Yao et al. [58] evaluated the photodegradation of TET using 41.8 mW/cm² UV irradiation, obtaining an E_{EO} value of 8.65 kWh/m³/order. Yao et al. [58] obtained a higher rate constant than the one obtained in the present study by applying a light irradiation which was three times higher. Nevertheless, the E_{EO} was smaller which might be due to the type of reactor used by Yao et al. [58]. Yao et al. [58] used a mini-fluidic VUV/UV photoreaction system (MVPS), which has a high transmittance of UV light and a small distance from the lamp surface to the reaction solution.

Hassani et al. [59] studied the degradation of 20 mg/L CIP, obtaining a 0.0006 min⁻¹ reaction rate constant and 2048 kWh/m³/order E_{EO} for photo-degradation (UV) after 120 min, and a 0.0063 min⁻¹ reaction rate constant and 195.1 kWh/m³/order E_{EO} for photocatalysis with TiO₂. Lower energy consumptions were obtained in the present study. Yet the results demonstrate that UVC photocatalysis has a better performance and a lower energy consumption than photolysis. E_{EO} is proportional to the inverse of the reaction constant. Therefore, as photocatalysis has higher k_1 values than photolysis, the E_{EO} values are lower. Additionally, Hassani et al. [59] made a comparison in the use of UVA, UVB and UVC, revealing that UVC photogeneration of e^-/h^+ pairs is high which will generate more reactive radicals for the degradation of contaminants.

For the photo-degradation of SDZ, Yadav et al. [47] acquired a 0.001 min⁻¹ reaction rate and 922 kWh/m³/order E_{EO} while the present study obtained lower a E_{EO} value of 795.31 kWh/m³/order. The difference can be explained by the use of a different rated power in the two studies. Yadav et al. [47] used 56 W while preset study used 36 W. Moreover, for the photocatalytic degradation of SDZ with TiO₂, Yadav et al. [47] obtained a 0.006 min⁻¹ reaction rate and 138 kWh/m³/order E_{EO}. The present study obtained a lower E_{EO} value of 29.79 kWh/m³/order due to the higher reaction rate obtained (0.0141 min⁻¹). In addition, the current study used a larger reactor volume of 5.6 L while the reactor volume used in Yadav et al. [47] was of 2 L.

Kim et al. [60] obtained an E_{EO} value of 150 kWh/m³/order for the UVC degradation of 30 mg/L SMX at pH 4.63. Luo et al. [61] calculated an E_{EO} value of 0.0023 kWh/m³/order for the UV degradation of 5 mg/L SMX. There is a significant difference between the energy consumption values reported in the literature. However, when compared with the results obtained in the present study, UVC photocatalysis with TiO₂ demonstrated its potential as a good option for SMX removal from wastewater as it can attain high removals with a low energy consumption.

In addition, UVC photolysis and UVC/TiO₂ photocatalysis energy consumption for the degradation of SDZ and SMX obtained in the present study is comparable with other AOP studies. Yadav et al. [47] presented the E_{EO} values for the degradation of SDZ with different AOPs such as oxidation with persulfate (127.9 kWh/m³/order), photo-oxidation with persulfate (1.72 kWh/m³/order), and photocatalysis with TiO₂ supported in granular activated carbon (34.5 kWh/m³/order). Kim et al. [60] obtained a 0.46 kWh/m³/order for water radiolysis by gamma rays and 27.53 kWh/m³/order for ozone. Even though gamma rays have a low energy consumption, their potential use at industrial scale might not be feasible. Mirzaei et al. [62] evaluated the photocatalytic degradation of SMX by ZnO in the presence of fluoride ions by 10 W UVC irradiation, obtaining a rate constant of 0.099 min⁻¹ and a 3.88 kWh/m³/order E_{EO}. These comparisons show that photodegradation (UVC) and photocatalysis with TiO₂ (UVC/TiO₂) are promising techniques for VA removal.
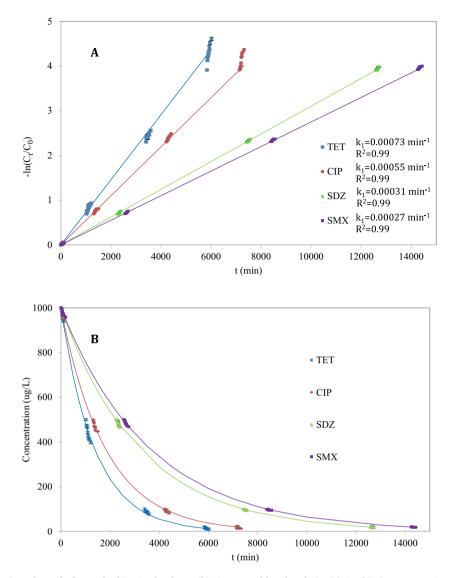
Fig. 5. (A) Linear representation of pseudo-first order kinetics for the antibiotic removal by photolysis. (B) Antibiotic concentration variation by photolysis along time. Error bars represent ± standard error of the mean.

Table 2
Comparative review from the last five years on the application of photolysis and photocatalysis with TiO_2 for the removal of VA.

TiO_2	Contaminant	Irradiance or lamp power	Light source	Irradiation time	Rate constant (min^{-1})	pH	References
0.2 g/L	10 mg/L TET	20 mW/cm^2	UV	120 min	0.02–0.04	–	Wu et al. [33]
0	10–40 mg/L TET	1.45 mW/cm^2	UV	15 days	0.0045–0.0014	6.2	Yun et al. [42]
0	500 µg/L TET	4 mW/cm^2	UVA/LED	30 min	0.01	6	Li and Hu, [43]
0.002 g/L					0.1		
0	20 mg/L CIP	10 mW/cm^2	UVA/LED	60 min	0.01	6	Li and Hu, [44]
0.1 g/L					0.22		
0	0.02 µg/L CIP	15 W	UVC	120 min	0.002	3	Salma et al. [1]
20.5 g/m^2 glass plate					0.006		
0	20 mg/L CIP	10 mW/cm^2	UV	8 h	0.003	–	Triquet et al. [45]
0.12 g/L				1 h	0.06		
0	500 µg/L SDZ	5.5 mW/cm^2	UVC	36 h	0.002	7.3	Loureiro dos Louros et al. [46]
0	1.5 mg/L SDZ	350 W	UV	150 min	0.02	7	Li et al. [21]
0	1 mg/L SDZ	28 W	UVC	120 min	0.001	–	Yadav et al. [47]
1 g/L					0.01		
0.05 g/L	400 µg/L SMX	$4.32 \cdot 10^3$ mWs/cm^2	UV	20 min	–	5.6	Cai and Hu, [2]
0	150 µg/L SMX	983 mW/cm^2	Solar simulator	4 h	0.002	8	Wang et al. [48]
0	200 µg/L SMX	0.5 mW/cm^2	UVC	16 min	0.03	6	Yuan et al. [26]
0.4 g/L					0.1		
1.6 g/L					0.5		

Fig. 6. Linear representation of Langmuir-Hinshelwood kinetics for the antibiotic removal by photocatalysis. (B) Antibiotic concentration variation by photocatalysis along time. Error bars represent ± standard error of the mean.
* Photocatalysis of SMX adjusted to a pseudo-first order kinetics because K = 0
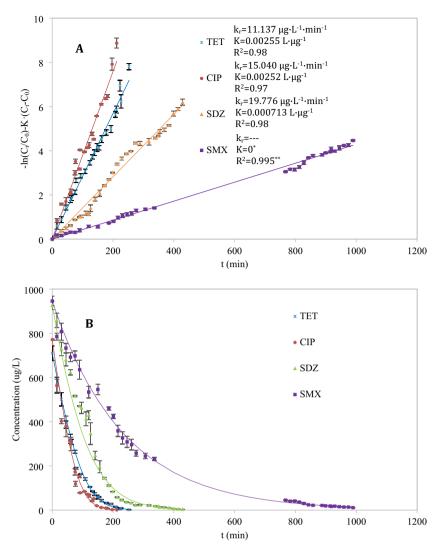** The linear adjust corresponds to a pseudo-first order kinetics because K = 0.

Table 3
Comparative review of the energy consumed for VA removal by photolysis and photocatalysis with TiO_2.

TiO_2 (g/L)	Contaminant	Irradiance or lamp power	Light source	Irradiation time	E_{EO} (kWh/m³/order)	pH	Rate constant (min⁻¹)	References
0	8.9 mg/L TET	41.8 mW/cm²	UV	12 min	8.65	7	0.0098	Yao et al. [58]
0	20 mg/L CIP	16 W	UV	120 min	2048	5	0.0006	Hassani et al. [59]
0.1					195.1		0.0063	
0	1 mg/L SDZ	56 W	UVC	240 min	922.22	–	0.001	Yadav et al. [47]
1		28 W		120 min	138		0.006	
0	30 mg/L SMX	6 W	UVC	15 min	1.5	4.63	–	Kim et al. [60]
0	5 mg/L SMX	10 W	UV	15 min	0.0023	8	0.36	Luo et al. [61]

4. Conclusions

Removal efficiencies, kinetics and energy consumption were evaluated for the photo-degradation (UVC) and photocatalytic-degradation with TiO_2 (UVC/TiO_2) of a mixture of four antibiotics at different initial concentrations. TET, CIP, SDZ and SMX proved to be photosensitive and capable of being removed by either photolysis or photocatalysis. Photocatalysis attained the higher degradation percentages. This study has analyzed for the first time the photolytic and photocatalytic degradation kinetics of VA over a wide range of concentrations, such as those found in real water samples, using a general equation for the whole set of concentrations analyzed and not using individual equations for each initial concentration which is a misconception found in the literature. Its limitation is that it is only applicable for the pH and temperature used in this study. The photolysis for the four veterinary antibiotics followed a first-order irreversible kinetic model. The photocatalysis of TET, CIP and SDZ followed a Langmuir-Hinshelwood kinetic model, and adsorption was considered as the limiting step. SMX followed a first-order irreversible kinetic model. The calculation of the electrical energy consumed by both processes showed that photocatalysis is energy efficient compared with other systems. These results are helpful to assess the extent of degradation of VAs in water treatment processes by photolysis and photocatalysis. UVC photocatalysis with TiO_2 was found to be efficient and cost-effective in the removal of VAs. Further investigations shall be done in the influence of different parameters such as ions and oxidants present in real water samples that

could enhance the photolytic and photocatalytic degradation of VAs.

Declaration of competing interest

Acknowledgements

References

[1] A. Salma, S. Thoröe-Boveleth, T.C. Schmidt, J. Tuerk, Dependence of transformation product formation on pH during photolytic and photocatalytic degradation of ciprofloxacin, J. Hazard. Mater. 313 (2016) 49–59, https://doi.org/10.1016/j.jhazmat.2016.03.010.

[2] Q. Cai, J. Hu, Decomposition of sulfamethoxazole and trimethoprim by continuous UVA/LED/TiO2 photocatalysis: decomposition pathways, residual antibacterial activity and toxicity, J. Hazard. Mater. 323 (2017) 527–536, https://doi.org/10.1016/j.jhazmat.2016.06.006.

[3] D. Cheng, H.H. Ngo, W. Guo, S.W. Chang, D.D. Nguyen, Y. Liu, Q. Wei, D. Wei, A critical review on antibiotics and hormones in swine wastewater: water pollution problems and control approaches, J. Hazard. Mater. 387 (2020), 121682, https://doi.org/10.1016/j.jhazmat.2019.121682.

[4] Y. Han, L. Yang, X. Chen, Y. Cai, X. Zhang, M. Qian, X. Chen, H. Zhao, M. Sheng, G. Cao, G. Shen, Removal of veterinary antibiotics from swine wastewater using anaerobic and aerobic biodegradation, Sci. Total Environ. 709 (2020), 136094, https://doi.org/10.1016/j.scitotenv.2019.136094.

[5] C. Kiki, A. Rashid, Y. Wang, Y. Li, Q. Zeng, C.P. Yu, Q. Sun, Dissipation of antibiotics by microalgae: kinetics, identification of transformation products and pathways, J. Hazard. Mater. 387 (2020), https://doi.org/10.1016/j.jhazmat.2019.121985.

[6] D. García, S. Bolado, G. Acién, R. Muñoz, E. Posadas, P. García-Encina, S. Blanco, Evaluation of the dynamics of microalgae population structure and process performance during piggery wastewater treatment in algal-bacterial photobioreactors, Bioresour. Technol. 248 (2017) 120–126, https://doi.org/10.1016/j.biortech.2017.06.079.

[7] Z. Huang, T. Wang, M. Shen, Z. Huang, Y. Chong, L. Cui, Coagulation treatment of swine wastewater by the method of in-situ forming layered double hydroxides and sludge recycling for preparation of biochar composite catalyst, Chem. Eng. J. 369 (2019) 784–792, https://doi.org/10.1016/j.cej.2019.03.136.

[8] K.J. Choi, H.J. Son, S.H. Kim, Ionic treatment for removal of sulfonamide and tetracycline classes of antibiotic, Sci. Total Environ. 387 (2007) 247–256, https://doi.org/10.1016/j.scitotenv.2007.07.024.

[9] M.J. Ahmed, Adsorption of quinolone, tetracycline, and penicillin antibiotics from aqueous solution using activated carbons: review, Environ. Toxicol. Pharmacol. 50 (2017) 1–10, https://doi.org/10.1016/j.etap.2017.01.004.

[10] Z. Fallah, E. Nazarzadeh, M. Ghomi, F. Ahmadijokani, in: Chemosphere Toxicity and Remediation of Pharmaceuticals and Pesticides Using Metal Oxides and Carbon Nanomaterials, 2021, p. 275, https://doi.org/10.1016/j.chemosphere.2021.130055.

[11] A. Mirzaei, Z. Chen, F. Haghighat, L. Yerushalmi, Removal of pharmaceuticals and endocrine disrupting compounds from water by zinc oxide-based photocatalytic degradation: a review, Sustain. Cities Soc. 27 (2016) 407–418, https://doi.org/10.1016/j.scs.2016.08.004.

[12] T.A. Ternes, J. Stüber, N. Herrmann, D. McDowell, A. Ried, M. Kampmann, B. Teiser, Ozonation: a tool for removal of pharmaceuticals, contrast media and musk fragrances from wastewater? Water Res. 37 (2003) 1976–1982, https://doi.org/10.1016/S0043-1354(02)00570-5.

[13] A. Fraiese, V. Naddeo, M. Prado, A. Cesaro, T. Zarra, H. Liu, V. Belgiorno, B.J. F, P. Ii, Removal of emerging contaminants in wastewater by sonolysis, photocatalysis and ozonation, Global NEST J. 21 (2018) 98–105, https://doi.org/10.30955/gnj.002625.

[14] M. Dolatabadi, M.T. Ghaneian, C. Wang, S. Ahmadzadeh, Electro-Fenton approach for highly efficient degradation of the herbicide 2,4-dichlorophenoxyacetic acid from agricultural wastewater: process optimization, kinetic and mechanism, J. Mol. Liq. 334 (2021), 116116, https://doi.org/10.1016/j.molliq.2021.116116.

[15] M. Dolatabadi, T. Świergosz, S. Ahmadzadeh, Electro-Fenton approach in oxidative degradation of dimethyl phthalate - the treatment of aqueous leachate from landfills, Sci. Total Environ. 772 (2021), https://doi.org/10.1016/j.scitotenv.2021.145323.

[16] S. Ahmadzadeh, M. Dolatabadi, Removal of acetaminophen from hospital wastewater using electro-Fenton process, Environ. Earth Sci. 77 (2018) 1–11, https://doi.org/10.1007/s12665-017-7203-7.

[17] M.P.C.A. Martínez-Huitle, Electrochemical oxidation of organic pollutants for wastewater treatment, Curr. Opin. Electrochem. 11 (2018) 62–71.

[18] J. Zambrano, B. Min, Electrochemical treatment of leachate containing highly concentrated phenol and ammonia using a Pt/Ti anode at different current densities, Environ. Technol. Innov. 18 (2020), https://doi.org/10.1016/j.eti.2020.100632.

[19] S. Ahmadzadeh, A. Asadipour, M. Pournamdari, B. Behnam, H.R. Rahimi, M. Dolatabadi, Removal of ciprofloxacin from hospital wastewater using electrocoagulation technique by aluminum electrode: optimization and modelling through response surface methodology, Process Saf. Environ. Prot. 109 (2017) 538–547, https://doi.org/10.1016/j.psep.2017.04.026.

[20] S. Ahmadzadeh, M. Dolatabadi, Electrochemical treatment of pharmaceutical wastewater through electrosynthesis of iron hydroxides for practical removal of metronidazole, Chemosphere 212 (2018) 533–539, https://doi.org/10.1016/j.chemosphere.2018.08.107.

[21] H. Li, L. Duan, H. Wang, Y. Chen, F. Wang, S. Zhang, Photolysis of sulfadiazine under UV radiation: effects of the initial sulfadiazine concentration, pH, NO3− and Cd2+, Chem. Phys. Lett. 739 (2020) https://doi.org/10.1016/j.cplett.2019.136949.

[22] D.N. Nguyen, H.M. Bui, H.Q. Nguyen, Heterogeneous photocatalysis for the removal of pharmaceutical compounds, in: Curr. Dev. Biotechnol. Bioeng, Elsevier B.V, 2020, pp. 161–183, https://doi.org/10.1016/B978-0-12-819594-9.00007-3.

[23] Y. Abdollahi, A.H. Abdullah, U.I. Gaya, S. Ahmadzadeh, A. Zakaria, K. Shameli, Z. Zainal, H. Jahangirianb, N.A. Yusof, Photocatalytic degradation of 1,4-benzoquinone in aqueous ZnO dispersions, J. Braz. Chem. Soc. 23 (2012) 236–240, https://doi.org/10.1590/S0103-50532012000200007.

[24] M.R. Eskandarian, H. Choi, M. Fazli, M.H. Rasoulifard, Effect of UV-LED wavelengths on direct photolytic and TiO2 photocatalytic degradation of emerging contaminants in water, Chem. Eng. J. 300 (2016) 414–422, https://doi.org/10.1016/j.cej.2016.05.049.

[25] S. Aoudj, N. Drouiche, A. Khelifa, Emerging contaminants remediation by heterogeneous photocatalysis, in: Emerg. Nanomater. Contam. Wastewater Adv. Treat. Technol, Elsevier Inc, 2019, pp. 245–275, https://doi.org/10.1016/B978-0-12-814673-6.00009-7.

[26] R. Yuan, Y. Zhu, B. Zhou, J. Hu, Photocatalytic oxidation of sulfamethoxazole in the presence of TiO2: effect of matrix in aqueous solution on decomposition mechanisms, Chem. Eng. J. 359 (2019) 1527–1536, https://doi.org/10.1016/j.cej.2018.11.019.

[27] P. Fern, J. Blanco, S. Malato, F.J.De Nieves, in: Application of the Colloidal Stability of TiO 2 Particles for Recovery and Reuse in Solar Photocatalysis 37, 2003, pp. 3180–3188, https://doi.org/10.1016/S0043-1354(03)00157-X.

[28] J. Zhao, J. Wang, L. Fan, E. Pakdel, S. Huang, X. Wang, Immobilization of Titanium Dioxide on PAN Fiber as a Recyclable Photocatalyst Via Co-dispersion Solvent Dip Coating, 2016, https://doi.org/10.1177/0040517516632479.

[29] K. Davididou, E. Hale, N. Lane, E. Chatzisymeon, A. Pichavant, J.F. Hochepied, Photocatalytic treatment of saccharin and bisphenol-a in the presence of TiO2 nanocomposites tuned by Sn(IV), Catal. Today 287 (2017) 3–9, https://doi.org/10.1016/j.cattod.2017.01.038.

[30] S.N. Ahmed, W. Haider, Heterogeneous photocatalysis and its potential applications in water and wastewater treatment: a review, Nanotechnology 29 (2018), 342001, https://doi.org/10.1088/1361-6528/aac6ea.

[31] J. Gomes, J. Lincho, E. Domingues, R.M. Quinta-Ferreira, R.C. Martins, N-TiO2 photocatalysts: a review of their characteristics and capacity for emerging contaminants removal, Water (Switzerland) 11 (2019) 373, https://doi.org/10.3390/w11020373.

[32] X. Zhou, J. Wang, C. Lu, Q. Liao, F.O. Gudda, W. Ling, Antibiotics in animal manure and manure-based fertilizers: occurrence and ecological risk assessment, Chemosphere 255 (2020), 127006, https://doi.org/10.1016/j.chemosphere.2020.127006.

[33] S. Wu, H. Hu, Y. Lin, J. Zhang, Y.H. Hu, Visible light photocatalytic degradation of tetracycline over TiO2, Chem. Eng. J. 382 (2020), 122842, https://doi.org/10.1016/j.cej.2019.122842.

[34] R. López-Serna, M. Petrović, D. Barceló, Development of a fast instrumental method for the analysis of pharmaceuticals in environmental and wastewaters based on ultra high performance liquid chromatography (UHPLC)-tandem mass spectrometry (MS/MS), Chemosphere 85 (2011) 1390–1399, https://doi.org/10.1016/j.chemosphere.2011.07.071.

[35] F.A. Amaringo Villa, Determinación del punto de carga cero y punto isoeléctrico de dos residuos agrícolas y su aplicación en la remoción de colorantes, Rev. Investig. Agrar. Ambient. 4 (2013) 27, https://doi.org/10.22490/21456453.982.

[36] A.T. Besha, Y. Liu, C. Fang, D.N. Bekele, R. Naidu, Assessing the interactions between micropollutants and nanoparticles in engineered and natural aquatic environments, Crit. Rev. Environ. Sci. Technol. 50 (2020) 135–215, https://doi.org/10.1080/10643389.2019.1629799.

[37] Y.Y. Peng, F. Gao, H.L. Yang, H.W.J. Wu, C. Li, M.M. Lu, Z.Y. Yang, Simultaneous removal of nutrient and sulfonamides from marine aquaculture wastewater by concentrated and attached cultivation of Chlorella vulgaris in an algal biofilm membrane photobioreactor (BF-MPBR), Sci. Total Environ. 725 (2020), https://doi.org/10.1016/j.scitotenv.2020.138524.

[38] A. Prakash, A. Verma, S. Goyal, P. Gauba, Remediation of antibiotics from the environment, J. Basic Appl. Eng. Res. 2 (2015) 633–636. http://www.krishisanskriti.org/jbaer.html.

[39] J. Li, M. Cui, Kinetic study on the sorption and degradation of antibiotics in the estuarine water: an evaluation based on single and multiple reactions, Environ. Sci. Pollut. Res. (2020), https://doi.org/10.1007/s11356-020-10194-4.

[40] B. Ohtani, Photocatalysis a to Z-what we know and what we do not know in a scientific sense, J. Photochem. Photobiol. C Photochem. Rev. 11 (2010) 157–178, https://doi.org/10.1016/j.jphotochemrev.2011.02.001.

[41] K. Vasanth Kumar, K. Porkodi, A. Selvaganapathi, Constrain in solving langmuir-hinshelwood kinetic expression for the photocatalytic degradation of auramine O aqueous solutions by ZnO catalyst, Dyes Pigments 75 (2007) 246–249, https://doi.org/10.1016/j.dyepig.2006.05.035.

[42] S.H. Yun, E.H. Jho, S. Jeong, S. Choi, Y. Kal, S. Cha, Photodegradation of tetracycline and sulfathiazole individually and in mixtures, Food Chem. Toxicol. 116 (2018) 108–113, https://doi.org/10.1016/j.fct.2018.03.037.

[43] S. Li, J. Hu, Photolytic and photocatalytic degradation of tetracycline: effect of humic acid on degradation kinetics and mechanisms, J. Hazard. Mater. 318 (2016) 134–144, https://doi.org/10.1016/j.jhazmat.2016.05.100.

[44] S. Li, J. Hu, Transformation products formation of ciprofloxacin in UVA/LED and UVA/LED/TiO2 systems: impact of natural organic matter characteristics, Water Res. 132 (2018) 320–330, https://doi.org/10.1016/j.watres.2017.12.065.

[45] T. Triquet, C. Tendero, L. Latapie, M.H. Manero, R. Richard, C. Andriantsiferana, TiO2 MOCVD coating for photocatalytic degradation of ciprofloxacin using 365 nm UV LEDs - kinetics and mechanisms, J. Environ. Chem. Eng. 8 (2020), https://doi.org/10.1016/j.jece.2020.104544.

[46] V. Loureiro dos Louros, C.P. Silva, H. Nadais, M. Otero, V.I. Esteves, D.L.D. Lima, Photodegradation of sulfadiazine in different aquatic environments – evaluation of influencing factors, Environ. Res. 188 (2020), https://doi.org/10.1016/j.envres.2020.109730.

[47] M.S.P. Yadav, N. Neghi, M. Kumar, G.K. Varghese, Photocatalytic-oxidation and photo-persulfate-oxidation of sulfadiazine in a laboratory-scale reactor: analysis of catalyst support, oxidant dosage, removal-rate and degradation pathway, J. Environ. Manag. 222 (2018) 164–173, https://doi.org/10.1016/j.jenvman.2018.05.052.

[48] Y. Wang, F.A. Roddick, L. Fan, Direct and indirect photolysis of seven micropollutants in secondary effluent from a wastewater lagoon, Chemosphere 185 (2017) 297–308, https://doi.org/10.1016/j.chemosphere.2017.06.122.

[49] M. Pelaez, A.A. de la Cruz, E. Stathatos, P. Falaras, D.D. Dionysiou, Visible light-activated N-F-codoped TiO2 nanoparticles for the photocatalytic degradation of microcystin-LR in water, Catal. Today 144 (2009) 19–25, https://doi.org/10.1016/j.cattod.2008.12.022.

[50] C. Zhao, M. Pelaez, X. Duan, H. Deng, K. O'Shea, D. Fatta-Kassinos, D.D. Dionysiou, Role of pH on photolytic and photocatalytic degradation of antibiotic oxytetracycline in aqueous solution under visible/solar light: kinetics and mechanism studies, Appl. Catal. B Environ. 134–135 (2013) 83–92, https://doi.org/10.1016/j.apcatb.2013.01.003.

[51] S. Malato, M.I. Maldonado, P. Fernández-Ibáñez, I. Oller, I. Polo, R. Sánchez-Moreno, Decontamination and disinfection of water by solar photocatalysis: the pilot plants of the plataforma solar de almeria, Mater. Sci. Semicond. Process. 42 (2016) 15–23, https://doi.org/10.1016/j.mssp.2015.07.017.

[52] A.L. Boreen, W.A. Arnold, K. McNeill, Photochemical fate of sulfa drugs in then aquatic environment: sulfa drugs containing five-membered heterocyclic groups, Environ. Sci. Technol. 38 (2004) 3933–3940, https://doi.org/10.1021/es0353053.

[53] G.H. Safari, M. Hoseini, M. Seyedsalehi, H. Kamani, J. Jaafari, A.H. Mahvi, Photocatalytic degradation of tetracycline using nanosized titanium dioxide in aqueous solution, Int. J. Environ. Sci. Technol. 12 (2014) 603–616, https://doi.org/10.1007/s13762-014-0706-9.

[54] E.O. Oseghe, A.E. Ofomaja, Study on light emission diode/carbon modified TiO2 system for tetracycline hydrochloride degradation, J. Photochem. Photobiol. A Chem. 360 (2018) 242–248, https://doi.org/10.1016/j.jphotochem.2018.04.048.

[55] S.K. Mondal, A.K. Saha, A. Sinha, Removal of ciprofloxacin using modified advanced oxidation processes: kinetics, pathways and process optimization, J. Clean. Prod. 171 (2018) 1203–1214, https://doi.org/10.1016/j.jclepro.2017.10.091.

[56] X. Xiang, L. Wu, J. Zhu, J. Li, X. Liao, H. Huang, J. Fan, K. Lv, in: Photocatalytic Degradation of Sulfadiazine in Suspensions of TiO 2 Nanosheets With Exposed (001) Facets 32, 2021, pp. 3215–3220.

[57] S.K. Alharbi, J. Kang, L.D. Nghiem, J.P. van de Merwe, F.D.L. Leusch, W.E. Price, Photolysis and UV/H2O2 of diclofenac, sulfamethoxazole, carbamazepine, and trimethoprim: identification of their major degradation products by ESI–LC–MS and assessment of the toxicity of reaction mixtures, Process Saf. Environ. Prot. 112 (2017) 222–234, https://doi.org/10.1016/j.psep.2017.07.015.

[58] H. Yao, J. Pei, H. Wang, J. Fu, Effect of Fe(II/III) on tetracycline degradation under UV/VUV irradiation, Chem. Eng. J. 308 (2017) 193–201, https://doi.org/10.1016/j.cej.2016.09.074.

[59] A. Hassani, A. Khataee, S. Karaca, Photocatalytic degradation of ciprofloxacin by synthesized TiO2 nanoparticles on montmorillonite: effect of operation parameters and artificial neural network modeling, J. Mol. Catal. A Chem. 409 (2015) 149–161, https://doi.org/10.1016/j.molcata.2015.08.020.

[60] T.H. Kim, S.D. Kim, H.Y. Kim, S.J. Lim, M. Lee, S. Yu, Degradation and toxicity assessment of sulfamethoxazole and chlortetracycline using electron beam, ozone and UV, J. Hazard. Mater. 227–228 (2012) 237–242, https://doi.org/10.1016/j.jhazmat.2012.05.038.

[61] S. Luo, Z. Wei, R. Spinney, Z. Zhang, D.D. Dionysiou, L. Gao, L. Chai, D. Wang, R. Xiao, UV direct photolysis of sulfamethoxazole and ibuprofen: an experimental and modelling study, J. Hazard. Mater. 343 (2018) 132–139, https://doi.org/10.1016/j.jhazmat.2017.09.019.

[62] A. Mirzaei, L. Yerushalmi, Z. Chen, F. Haghighat, J. Guo, Enhanced photocatalytic degradation of sulfamethoxazole by zinc oxide photocatalyst in the presence of fluoride ions: optimization of parameters and toxicological evaluation, Water Res. 132 (2018) 241–251, https://doi.org/10.1016/j.watres.2018.01.016.